


# Investigation of damage detectability in composites using frequency-based classification of Acoustic Emission measurements

Journal Title  
XX(X):1–12  
©The Author(s) 2016  
Reprints and permission:  
sagepub.co.uk/journalsPermissions.nav  
DOI: 10.1177/ToBeAssigned  
www.sagepub.com/  


Sebastian Felix Wirtz, Nejra Beganovic, Dirk Söffker

## Abstract

Advances in composite technology led to the substitution of conventional, metallic construction material by composites. However, the more widespread application of composites is currently restricted by complex fracture mechanisms, which are not well understood. One approach to overcome this challenge are Structural Health Monitoring (SHM) systems which provide several information on the current system state as well as state-of-health in real-time. In this context, reliability assessment of SHM systems is currently an open issue. The reliability of conventional non-destructive testing (NDT) systems is evaluated, measured, and partly standardized using widely accepted methods such as the Probability of Detection (POD) rate. Frequently, the  $a_{90|95}$  value, which is determined from POD curves, is used as a performance measure indicating the minimum damage size that is detected with a probability of 90 % and 95 % confidence. In contrast to NDT, SHM involves additional data analysis steps, i.e. statistical pattern recognition, where the classification results are also subject to uncertainty. Because similar methods are not available, the reliability of SHM systems is usually not quantified. To investigate influences on the classification performance, experiments were conducted. In particular, the effect of variable loading conditions and the evolution of damage over time are considered. To this end, AE measurements were performed while specimens of composite material were subjected to different cyclic loading patterns. Here, AE refers to elastic stress waves in the ultrasound regime, which emerge from the structure on damage initiation and propagation. Furthermore, a frequency-based damage classification scheme for AE measurements is proposed. Time-frequency domain features are extracted from the measurement signals using Short-Time Fourier Transform (STFT). Classification is performed using Support Vector Machine (SVM). Both choices serve as typical examples to discuss the effects which apply equally to other approaches. Experimental results presented in this paper regarding fault diagnosis and discrimination of delamination, matrix crack, debonding, and fiber breakage in CFRP material indicate strong dependences of the classification performance on loading conditions. Due to variability in the results, a direct and reliable relationship could not be established under identical test conditions. Concluding from the experimental results the question raises, which classification approaches, testing conditions, measurement devices, and filters are able to provide reliable statements about the actual damage state.

## Keywords

Acoustic Emission (AE), Support Vector Machine (SVM), Composite, Probability of Detection (POD), Reliability, Classification, Non-destructive Testing (NDT)

## Introduction

The recent rise of composites is owed to their beneficial properties, such as fatigue strength, impact resistance, and lightweight, resulting from their sophisticated structure. Today, the more widespread use of composites is restricted for several reasons. Compared to metallic materials, composites lack the pronounced ductile behavior.<sup>1</sup> Furthermore, composites form a complex system defined by the

constituent materials properties, geometry, and distribution,

---

Chair of Dynamics and Control,  
University of Duisburg-Essen,  
47048 Duisburg, Germany

### Corresponding author:

Dirk Söffker, University of Duisburg-Essen, 47048 Duisburg, Germany.  
Email: soeffker@uni-due.de

whereas metals are generally assumed to exhibit homogeneous mechanical properties.<sup>2</sup> Therefore, complex micro-mechanical fracture mechanisms are observed.<sup>1</sup> Structural Health Monitoring (SHM) systems are proposed to overcome these challenges and to ensure equal safety and reliability of composite structures.<sup>3</sup> This includes that the SHM system applied has to ensure reliable measurements and conclusions regarding the actual system state.

A definition of SHM is given by Farrar and Worden as “the process of implementing a damage identification strategy for aerospace, civil, and mechanical engineering”.<sup>4</sup> In general, the goal of such a strategy is to establish a surveillance system that is capable of continuously monitoring a technical system or structure. This enables advanced maintenance strategies, i.e. condition-based maintenance, which leads to an increase in reliability of technical systems.<sup>5</sup> In this context, methods for Nondestructive Evaluation (NDE) are employed. In particular, Acoustic Emission (AE) technique, which is a passive, wave-propagation-based NDE method, gained attention for in-situ monitoring recently. In general, AE refers to the phenomenon of elastic waves generated in the ultra-sound regime due to the sudden release of energy. These elastic waves emerge from distinct sources within a structure at frequencies between 10 kHz and 1 MHz.<sup>6</sup> In particular, this occurs on initiation and propagation of damage or due to external impact loads. Consequently, AE monitoring should be applied while the structure is loaded.

Sources of AE are manifold. In composites, only distinct types of damage are observed as the result of underlying micro-mechanical fracture mechanisms. In particular, these are delamination, matrix crack, fiber breakage, and debonding.<sup>7</sup> Whereas debonding merely describes the loss of adhesion between fiber and matrix material, delamination denotes the separation of layers in laminated materials.<sup>3</sup> The resulting AE waveforms are characteristic to the particular source mechanism and, hence, AE measurements can be utilized to identify the corresponding fracture mechanism, which has already been shown in several case studies.<sup>3;8-11</sup> For this purpose, modal analysis as well as time and frequency domain based approaches are distinguished.

Regarding modal properties of the AE waveforms, corresponding fracture mechanisms can be identified based on physical interpretation of the source motion. In thin plates, these waveforms propagate as guided waves, which can be described by means of Lamb wave theory.<sup>11</sup> Accordingly, two distinct wave modes – flexural and extensional waves – exist. These are promoted by either in-plane or out-of-plane source motion, respectively.<sup>12</sup> According to Prosser and Gutkin et al., the extensional wave mode is usually observed

at higher frequencies and exhibits faster propagation velocities than flexural waves.<sup>12;13</sup> Furthermore, this wave mode is symmetric and non-dispersive. In contrast, flexural waves are antisymmetric, propagate at lower velocities and are highly dispersive. In general agreement, several authors reported in-plane motion to be associated with fiber breakage<sup>3;9</sup> and matrix crack.<sup>9;11</sup> These damage mechanisms promote high frequency extensional waves. In contrast, delamination is governed by out-of-plane motion and thus promotes the flexural waves in the material generating low-frequency signals.<sup>3;9;11</sup>

For the purpose of automated damage classification, several statistical properties of the AE signals – referred to as features or descriptors – that can be calculated from both time and frequency domain, are frequently used. Typically, time domain features are used for the analysis of AE measurements.<sup>13-15</sup> However, time domain features are strongly dependent on the experimental conditions, whereas the frequency content is not affected. Particularly, the AE amplitude is subject to variable attenuation depending on the propagation path.<sup>11</sup> Thus, the frequency spectrum of AE signals is considered a more reliable descriptor of AE sources.<sup>9</sup>

To identify characteristic frequencies of distinct AE source mechanisms, peak frequency analysis was applied by several researchers.<sup>10;16;17</sup> De Groot et al.<sup>16</sup> identified damage-specific signatures of 4 different micro-mechanical damage modes namely matrix crack [90 kHz, 100 kHz], debonding [240 kHz, 310 kHz], fiber breakage [ $> 300$  kHz], and fiber pull-out [180 kHz, 240 kHz] in CFRP material in terms of peak frequencies. Similarly, Hamdi et al. identified matrix crack [30 kHz, 90 kHz], debonding [30 kHz, 170 kHz], and fiber breakage [300 kHz, 420 kHz] as distinct classes of micro-mechanical damage in composites using Hilbert Huang Transform (HHT).<sup>10</sup> To identify characteristic peak frequencies and to track damage accumulation under different experimental conditions Bussiba et al. used STFT. Based on their experimental results, three characteristic frequencies were identified, which correspond to the damage mechanisms matrix crack (140kHz), debonding (300kHz), and fiber-breakage (405kHz).<sup>17</sup> Moreover, mechanical thresholds for the onset of AE activity were determined, indicating that no damage occurs below these threshold values.<sup>17</sup>

Damage characterization task is most frequently considered as classification problem. Pattern recognition algorithms are a suitable method to address this type of problem.<sup>18</sup> Here, statistical learning theory is employed to determine the

mapping between class labels and input values. In the supervised case, a representative set of training data is used to generate the statistical model. Most frequently used classifier algorithms are K-Nearest Neighbor (KNN), Artificial Neural Network (ANN), and Support Vector Machine (SVM). Das et al. stated, that SVMs are a suitable method to identify damage modes in composites.<sup>19</sup> Here, joint time-frequency transformation was performed prior to the classification to extract damage specific features.

A generic SHM system is composed of a measurement chain, where principles of NDT are employed, and a signal processing chain. According to the statistical pattern recognition paradigm, damages are detected by means of classification.<sup>4</sup> To realize SHM systems in practice, a suitable and therefore well defined reliability of the classification must be achieved. This includes high detection rates as well as low false-alarm rates, so that the system can be accepted. Furthermore, the surveillance system should be robust against external disturbances.

The reliability of conventional NDT methods is frequently assessed using Probability of Detection (POD) as a probabilistic approach, which provides a measure of the reliability of an NDT method.<sup>20</sup> The POD curve describes the likelihood that a certain flaw is detected as a function of flaw characteristic  $a$  such as size or depth. These POD curves can be computed directly from experimental data, where two approaches are distinguished. In case of binary response of the inspection system hit/miss analysis is employed, whereas  $\hat{a}$  vs.  $a$  approach can be used if continuous output  $\hat{a}$  of the inspection system is available.<sup>20</sup> Commonly the  $a_{90|95}$  value is determined from the POD curve as performance measure of the inspection system.<sup>21</sup>

The performance evaluation of a classifier is usually based on a set of testing data with known class labels. Here, the classifier output and true class labels are compared by means of a confusion matrix. From the confusion matrix, different scores, such as accuracy, sensitivity, and specificity are extracted to assess the performance of classification algorithms.<sup>22</sup> Here, sensitivity denotes the detection rate, whereas false alarm rate is the complement of the specificity of a classifier. In general, improved detection rates can only be achieved at the cost of increasing false alarm rates. The principle relationship between detection and false alarm rate is described by ROC curve,<sup>23</sup> which compares the detection and false alarm rate of a classifier. In the context of classification algorithms, the POD is understood as the true positive rate, which is also known as the sensitivity of a classifier.<sup>22:24</sup> However, these measures only provide

quantification of model performance with respect to a specific set of testing data.

Due to conceptual differences between SHM and NDE, reliability of SHM systems is usually not quantified. In order to determine the POD curve of a NDE inspection technique, fixed decision threshold of the sensor response  $\hat{a}$  is determined using model (calibration) specimens under controlled laboratory conditions.<sup>25</sup> Due to the in-service application of SHM, damages evolve over time and exclusion of disturbances is generally not possible.<sup>26</sup> Consequently, the sensor output is compared to a baseline signal for damage detection, where deviations cannot be readily attributed to damage due to in-situ effects and hence, require appropriate interpretation.<sup>25</sup> Influencing factors of NDE systems are for instance reported as testing equipment and procedures, material and geometry of test specimens, and properties of the particular defect.<sup>20</sup> In contrast to this, SHM systems are reportedly affected by loading conditions,<sup>26</sup> temperature,<sup>25</sup> and sensor degradation.<sup>25</sup> For instance, Gagar et al. reported strong dependence of AE activity on the particular loading conditions using aluminum specimens under cyclic loading patterns.<sup>27</sup> Furthermore, Schubert Kabban et al. mentioned, that the assumption of independent observations is not feasible in case of SHM systems, because measurements are performed at high acquisition rates to determine the current state-of-health in real-time leading to several dependent observations.<sup>21</sup>

In this work, experiments were conducted to investigate the impact of variable loading conditions on the reliability of SHM systems. Due to practical relevance, diagnosis of a composite structure was chosen to showcase SHM implementation. A mechanical test rig was used to simulate a load bearing structure of composite material while AE measurements are performed. Furthermore, a statistical pattern recognition approach using STFT-based feature extraction and SVM-based classification of the measurement results is proposed as example. Finally, the performance of the classification results is evaluated with respect to damage evolution and variable loading conditions using probability estimation. In the following sections, the experimental procedure is introduced, the measuring chain as well as the employed signal processing techniques are described. Hereafter experimental results of the proposed procedure are presented and discussed with respect to reliability considerations of SHM applications. Finally, the main conclusions from the experimental results are summarized.

## Experiments

In the context of this work, experiments were performed to investigate the effect of loading conditions and damage evolution on the reliability of automatic damage classification. To this end, a test rig is used to subject specimens of composite material to cyclic loading patterns while AE measurements are performed for diagnostic purposes. In this section, the mechanical test rig, data acquisition hardware, and methods used for signal processing are briefly described.

### Mechanical test rig

In order to simulate a in-service, load-bearing structure, a mechanical test rig was developed, which is used to subject specimens of composite material to cyclic loading patterns. The major components of the test-rig are presented in figure 1. The frame construction of the test rig consists

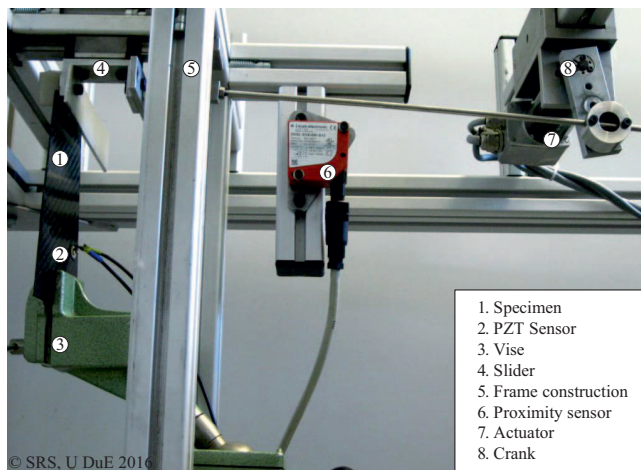


**Figure 1.** Components of the mechanical test rig, SRS U DuE

of aluminum profiles, having a vise attached to fixate the specimen during testing. Furthermore, a slider-crank mechanism, which converts the rotational motion of the motor into linear displacement, is used to apply bending load by deflecting the specimens tip. For actuation of the test rig, a servo-controlled BLDC motor manufactured by Maxon motors is mounted on the aluminum frame. The BLDC motor is driven by a servo-amplifier of the type Maxon 4-Q-EC, providing control of the motor current. Setpoint values for the motor current are read from analog input in the range of 0 – 5 V. Moreover, a laser proximity sensor of the type ODSL9 by Leuze is used for contactless displacement measurement. The sensor provides a maximum resolution of 0.1 mm in the maximum measuring range of 50 – 650 mm of distance. Here, the measuring range was configured to an interval of 65 mm. The motion control algorithm is implemented using LabView and a National Instruments USB I/O board of the type NI USB 6229, featuring 32 analog

input and 4 analog output ports of 16 bit resolution. To drive the actuator, output values are computed by the control algorithm according to the actual displacement of the tip, which is captured by the laser proximity sensor.

### Data acquisition

The AE technique relies on the measurement of surface waves, such as Rayleigh and Lamb waves.<sup>28</sup> Therefore, small surface displacements need to be detected to record AE. Consequently, signals obtained from AE measurements are characterized by high frequency content and low amplitudes. Hence, high sensitivity of the measuring system and high acquisition rates are crucial.<sup>12</sup> For instance, Al-Jumaili et al. used a sample rate of 5 MHz for AE monitoring.<sup>29</sup>

A generic measuring chain for AE applications consists of sensors, amplifiers, and data acquisition hardware.<sup>6</sup> To record surface waves generated by AE, a surface-mounted, piezoelectric acceleration sensor is employed, because these are robust and well-established technology in the field of AE. It consists of a disk-shaped piezoceramic element of 0.55 mm thickness and Ø10 mm in diameter featuring a resonant frequency of 3.6 MHz. As bonding agent, cyanoacrylic glue was used to attach the sensor to the specimen. This couplant was reported to provide good reproducibility compared with other couplants.<sup>30</sup> Furthermore, the stiff bonding improves transmission properties of in-plane wave modes and provides permanent bonding of the sensor to the structure.<sup>31</sup> To capture the low-power sensor response produced by the piezoelectric element, the sensor is connected to a pre-amplification device which drives the A/D conversion hardware. For data acquisition a Field-Programmable-Gate-Array (FPGA) board offering 16 bit resolution at a maximum sample rate of 25 MHz is used. A sample rate of 4 MHz was chosen as suitable trade-off between resolution and technical requirements. The waveforms were acquired continuously.

Examples of acquired waveforms are presented in figures 2 and 3, respectively. Here, the time-series data as well as joint time-frequency domain representation using continuous wavelet decomposition are presented. The event shown in figure 2 is considered as representative of delamination. The source motion of this fracture mechanism is mainly characterized by out-of-plane displacement. According to literature, AE events of high amplitude exhibiting a dominant flexural wave mode are presumably associated with delamination.<sup>3;9;11</sup> Furthermore, these waveforms are highly dispersive and show long durations.<sup>12</sup> In general agreement, the frequency content of delamination is reported

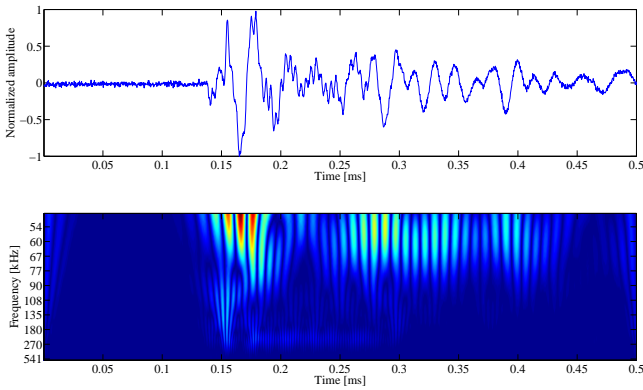


**Figure 2.** Time and time-frequency representation of delamination events

in the lower frequency band of the ultrasonic regime at frequencies of [50 kHz, 150 kHz] according to Gutkin et al.,<sup>13</sup> whereas Hamdi et al. reported lower frequencies of delamination events in the range of [30 kHz, 90 kHz].<sup>10</sup> In contrast to this, the AE waveform presented in figure 3 is attributed to the class of fiber breakage. This type of damage occurs, if the maximum strain of the fiber is exceeded due to excessive deformation of the matrix material. Here, the rapid redistribution of stress due to the reinforcement failure primarily activates in-plane source motion. Therefore, high frequency extensional modes featuring short rise time and duration are associated with fiber breakage.<sup>3,9</sup> According to literature, the peak frequency is localized at frequencies above 300 kHz. Maximum frequency range of fiber-breakage was reported by Bohse et al. at frequencies in the range of [350 kHz, 700 kHz],<sup>32</sup> whereas the lowest interval was reported as [300 kHz, 400 kHz] by Suzuki et al.<sup>33</sup>

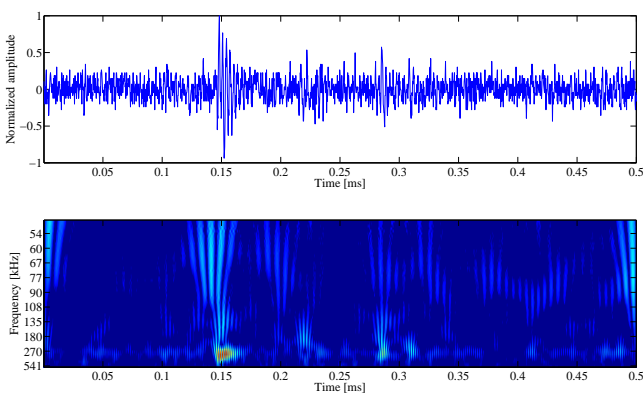


**Figure 3.** Time and time-frequency representation of fiber breakage events

### Time-frequency analysis

The physical meaning, and hence interpretability of a measurement signal is closely linked to the actual representation. Usually, damage information is not readily

available from the time domain representation of a signal.<sup>34</sup> Therefore, feature extraction is performed and damage-specific signatures are identified for diagnostic purposes. Furthermore, it can provide compression of the acquired data. Signal transforms, such as Short-Time Fourier Transform (STFT), Wavelet Transform (WT), and Hilbert Huang Transform (HHT) are mathematical methods which can be used to study AE signals in the frequency domain.<sup>10</sup>

In the context of this work, frequency domain features of transient AE bursts are determined by means of STFT, which provides acceptable data compression rates due to windowing. However, this method is limited by the trade-off between time and frequency resolution, which is related to the uncertainty principle. Here, the lower bound of time and frequency resolution is given as

$$\Delta\tau \cdot \Delta w \geq \frac{1}{2},$$

where  $\Delta\tau$  and  $\Delta w$  denote time- and frequency resolution, respectively.<sup>36</sup> Increased window sizes lead to improvement in frequency resolution and decrease in time resolution, respectively. Furthermore, considering a particular window size, the time-frequency resolution is fixed.

### Pattern recognition

The Support Vector Machine (SVM) is a supervised classification algorithm, which has emerged from the original research of Vapnik in the late 1970s. Due to its high accuracy and good generalization performance,<sup>37</sup> SVM is widely used in various pattern recognition tasks such as image classification,<sup>38</sup> data mining,<sup>39</sup> and classification of faults in rotating machinery.<sup>40</sup> The SVM follows the supervised machine-learning approach, so that labeled training data must be provided to the algorithm. The goal of the training algorithm is to determine an optimal decision function in terms of a separating hyperplane which geometrically separates different classes according to the training data. These data points, which are located closest to the separating hyperplane – referred to as support vectors – are of significant importance, because they “contain all the information to design the classifier”.<sup>41</sup> To obtain a solution for training data, where different classes are not linearly separable, kernel functions are employed to perform a linear transformation of the feature space.<sup>37</sup> From a practical point of view, Hsu et al. advise using a Radial Basis Function (RBF) kernel as a first choice. The stated reason is that there are fewer numerical difficulties to be faced compared to other kernel functions.<sup>42</sup>

## Results

In this work, experiments were conducted to investigate the performance of the proposed classification scheme and related dependencies with respect to the load applied. To this end, AE measurements were conducted on multiple specimens while they were subjected to cyclic loading patterns. Here, the loading of the structure promotes micro-mechanical fracture of the material as a result of damage propagation and, hence, activates characteristic AE source mechanisms. Statistical pattern recognition is employed to determine the underlying fracture mechanisms from the acquired AE waveforms. However, AE is an in-situ inspection technique, that is, damage detection will only be possible on initiation or propagation and is therefore non-deterministic.<sup>43</sup> Moreover, considering structures under load, additional variability of the classification results may be related to the evolution individual defects. Furthermore, loading conditions reportedly affect the activation of AE source mechanisms in aluminum specimens, which has already been found by Gagar et al.<sup>27</sup> Therefore, measurements are performed at different points in time, while keeping the excitation motion constant to study the spread of classification performance over time due to statistical scattering and damage evolution. Moreover, measurements are performed using variable loading conditions as well as to investigate the impact of loading conditions on the classification performance.

Classification of the acquired waveforms was performed using LIBSVM library.<sup>44</sup> Here, probability estimates were computed by the SVM in addition to the predicted class labels, as described by Chang and Lin.<sup>44</sup> The probability estimation is a measure for the likelihood that a specific instance is actually a member of the predicted class. Hence, probability estimates can be considered to assess the reliability of the classification results. To generate a suitable SVM model, example datasets are used, which are obtained during several fracture tests. For the purpose of model generation and evaluation, a labeled dataset containing true class labels are constructed based on the results from several fracture tests. In particular, three-points bending as well as indentation flexure tests were employed. Reportedly, each of the damage modes can be identified in connection with three points bending,<sup>10</sup> whereas indentation flexure test promote primarily delamination.<sup>29</sup> From these experiments, several characteristic peak frequencies could be identified. The lowest characteristic frequency was assigned to delamination exhibiting peak frequencies in the spectrogram at approximately 45 kHz, which is

in accordance with the findings of several authors.<sup>10;13</sup> Furthermore, matrix crack is attributed to peak frequencies of 95 kHz, which is in line with multiple reports from literature.<sup>7;10;16;45</sup> Moreover, debonding is presumably associated to frequencies of approximately 245 kHz, which is in accordance with literature.<sup>7;10;13;16</sup> Finally, the maximum frequency of 300 kHz is assigned to fiber breakage, which is located at the lower end of frequencies being reportedly related to fiber breakage.<sup>10;16;45</sup> From each of the classes (i) delamination, (ii) matrix crack, (iii) debonding, and (iv) fiber breakage, 60 representative samples of AE were selected carefully to construct a dataset for SVM training. During SVM model generation, this dataset was randomly split into training and testing data. The training dataset was composed out of 40 samples each, while the remaining samples were used for classifier testing. Here, a RBF kernel was used, as proposed by Hsu et al. where optimal classifier parameters  $C$  and  $\gamma$  were determined with respect to accuracy by means of grid-search.<sup>42</sup> Performance measures are summarized in table 1.

**Table 1.** SVM model performance

Class	Accuracy	Specificity	Sensitivity
Delamination	0.990	1.000	0.9500
Matrix crack	0.950	1.000	0.750
Debonding	0.980	1.000	0.900
Fiber breakage	0.990	0.988	1.000

In general, good classification performance is achieved according to the testing data. Here, each class achieves high accuracies indicating only few classification errors. With respect to accuracy, best performance is achieved in conjunction with delamination and fiber breakage. Furthermore, high values for sensitivity and specificity indicate high detection rates and low false alarm rates, respectively. Considering specificity, which denotes the complement of false alarm rate, no false detection occurred on the training data, except for fiber breakage. Here, improved detection rate is achieved at the cost of reduced specificity. Minimum detection rate of 0.75 is achieved in connection with matrix crack.

During the cyclic loading experiments, coupon shaped specimens of the dimension 75 mm × 175 mm × 1.8 mm were used. The specimens were manufactured from carbon fiber/epoxy composite material consisting of three layers of [90°/0°/90°] unidirectional layup patterns and two woven carbon/epoxy prepregs. Furthermore, similar initial damage was introduced to each specimen by means of three points bending, because a strain-threshold must be exerted to initiate AE activity in bending tests.<sup>17</sup> Using

carbon fiber/polymer composites, a significant fraction of the breaking load needs to be applied to give rise to micro-mechanical fracture due to the high bending elasticity of the material. According to Hamstad,<sup>46</sup> only low AE activity is detected at 90% of breaking load if undamaged composite material is subjected to cyclic bending load. Therefore, specimens containing initial damage were used in cyclic bending experiments.

### Constant excitation

To investigate the spread of the classification results over time, the excitation motion was kept constant and several measurements were performed at different points in time. Each series of measurements covers 20 min of time, while data acquisition was initiated every 5 min for a duration of 2 s. Accordingly, 5 datasets were recorded per test series. The results of two measurement series subjecting a single specimen to two different excitation motions of (a) [8mm, 4 Hz] and (b) [18 mm, 5 Hz], are presented. Three classes (delamination, matrix crack, and debonding) are considered. To assess the reliability of the classification results, mean values of the probability estimation shown in figure 4 are considered.

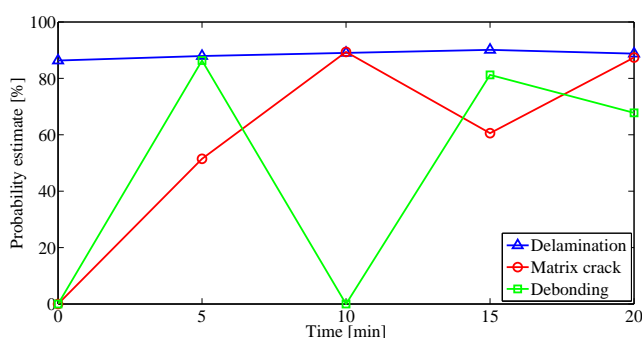


**Figure 4.** Mean values of the probability estimation over time (a)

Here, the specimen was subjected to excitation motion (a), which is characterized by small amplitudes and intermediate frequency of the loading pattern. In this case, the best results are achieved in connection with delamination events. In most of the cases, the highest probability estimates are achieved between 80 % and 90 %. Also, maximum probability estimate of 90% is achieved on this class after 15 minutes of the experiment. Moreover, delamination provides the minimum spread among the mean probability estimation which amounts to 4%. In contrast, the lowest probability estimation of 51 % can be observed in connection with matrix crack after 5 minutes. Furthermore, the maximum spread of the probability estimates of up to 38 % is observed in connection with matrix crack. Despite identical testing

conditions, damages can not be detected within each of the measurements. In particular, matrix crack and debonding are not detected within the first dataset. Moreover, debonding is not detected within the measurement performed after 10 minutes of the experiment. Presumably, this is attributed to the non-deterministic nature of the inspection method. From the absence of positive decision of the classifier it is concluded, that the particular source-mechanisms was not activated during the measurement.

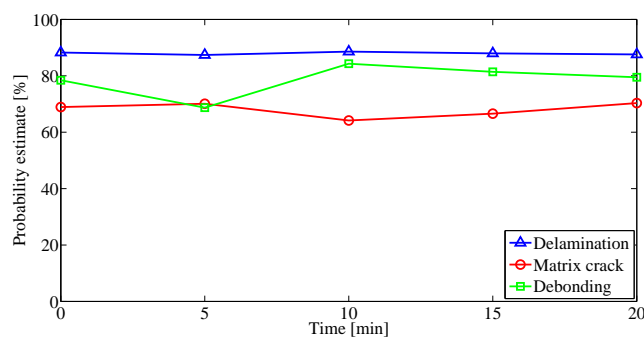


**Figure 5.** Mean values of the probability estimation over time (b)

Different results were obtained using controlled excitation motion (b), which provides increased load intensity. The results are presented in figure 5. Here, delamination provides the best classification performance, which is in accordance with the results obtained with excitation motion (a). In line with the results of excitation motion (a) maximum and minimum probability estimation of 89 % and 64 % are observed in connection with delamination and matrix crack, respectively after 10 minutes of operation. However, compared, to the results of excitation (a), the overall classification performance could be improved by using increased intensity of the loading pattern. In contrast to the results obtained in connection with loading pattern (a), all the damage modes could be detected within each measurement. Moreover, increased excitation amplitude and frequency lead to more homogeneous results, which is indicated by reduced spread of the probability estimation. The maximum and minimum spread of only 15 % and 1 % could be observed connection with the classes of debonding and delamination, respectively.

The main conclusion to be drawn from these experiments is that for a given specimen, the results obtained remain constant, so that during operation and test time, no additional fault (crack) development is observed. This is important, because it excludes related effects for the further experiment series to be reported in the sequel. Nevertheless, scattering of the classification performance is observed among different points in time. Furthermore, comparing the maximum spread

of the probability estimate achieved using excitation motion (a) and (b), reduction from 38 % to 15 % is observed indicating the dependence of classification reliability on loading conditions. Therefore, detailed investigation of the effect of loading conditions on the classification performance are presented.

### *Variable excitations*

To investigate the effect of the loading conditions on the classification performance, specimens of composite material were subjected to different cyclic loading patterns. To this end, AE measurements were performed while subjecting each of the specimens to any pair of the frequencies [2 Hz 3 Hz 4 Hz 5 Hz 6 Hz] and amplitudes [6 mm 9 mm 12 mm 15 mm 18 mm]. Hence, 25 datasets were acquired per specimen. During each measurement, data was acquired for 1.25 s. Furthermore, each series of measurements follows the identical sequence. The first measurement was carried out using the lowest excitation amplitude and frequency of [6 mm 2 Hz]. Hereafter, the frequency of the excitation motion was increased stepwise up to 6 Hz prior to increasing the excitation amplitude.

The classification results of each series of measurement performed on specimens S-I – S-III are summarized in table 2. Similar to the previous experiments, mean values of the probability estimation are computed from each dataset. From these results contour plots are rendered to illustrate the dependence of probability estimation on the excitation motion. Here, the probability estimation is plotted on a color scale while the x- and y-axis denote the amplitude and frequency of the excitation motion, respectively. Damage detection with a high probability estimate is denoted by a red shade. In case that no damage was detected, the probability estimation was set to 0, which corresponds to a dark blue shade.

Best results are achieved in connection with delamination. Except for specimen S-I, this damage mode is detected at any of the excitations providing high probability estimation. In many cases, high probability estimation above 90 % is achieved. In contrast, similar results are achieved for specific excitations in case of matrix crack, debonding, and fiber breakage. Furthermore, it is observed that improved probability estimation of delamination is achieved with the smallest amplitude of 6 mm in case of specimen S-II. However, in connection with specimen S-I delamination remained undetected at excitations of this particular amplitude and frequencies of 5 Hz and 6 Hz.

Regarding matrix crack events, a strong dependency between the loading pattern and damage detection as well as

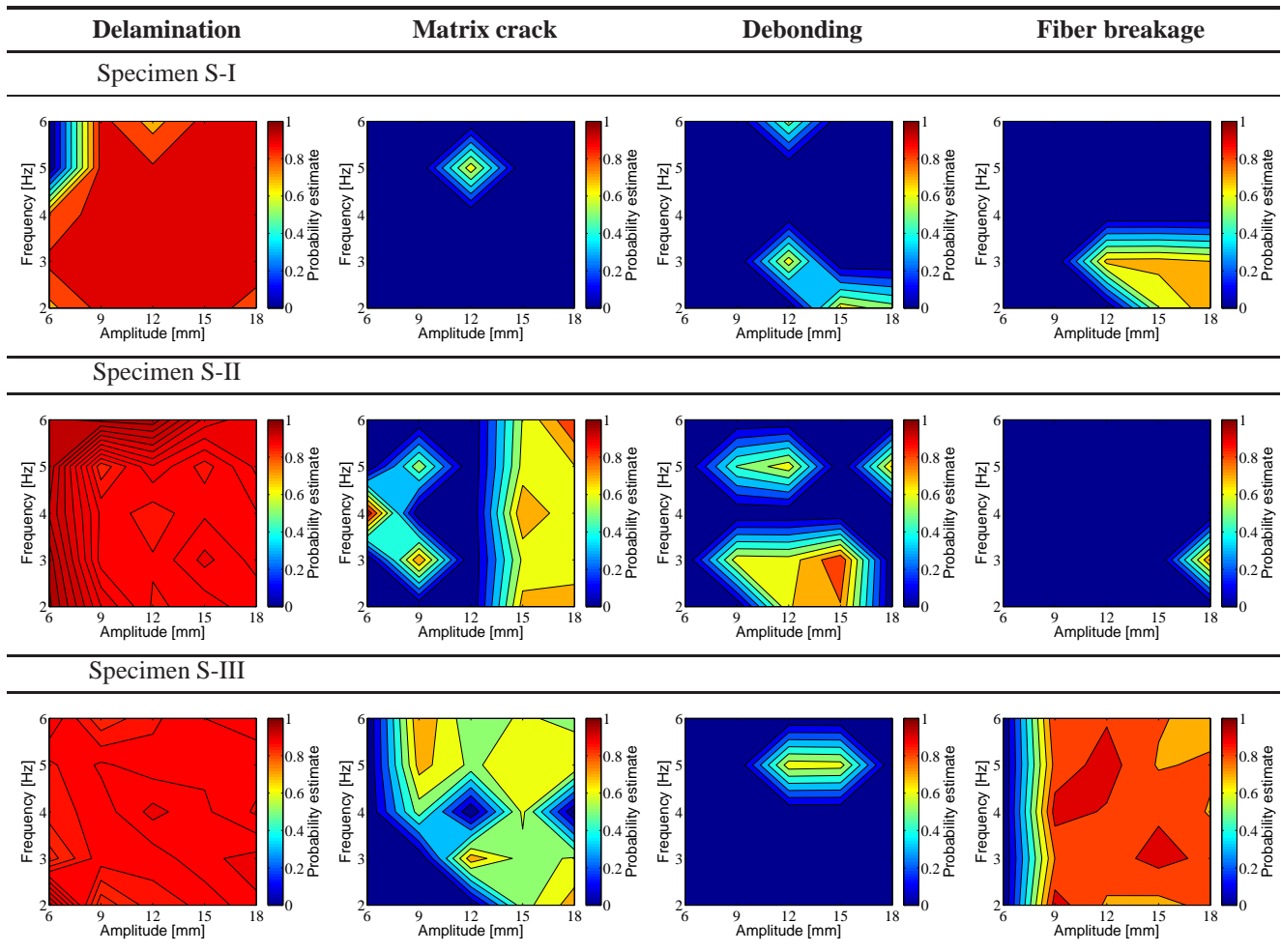
the corresponding estimated probability of the classification result is observed. Considering specimen S-II, maximum probability estimation is achieved using excitation motion of [6 mm, 4 Hz] showing minimum amplitude. In contrast to this, matrix crack was not detected at maximum excitation amplitude in case of the particular excitation motion of [18 mm 4 Hz] considering specimen S-III. Here, matrix crack could be detected at excitation amplitudes of 12 mm, whereas at this amplitude it was not detected throughout the measurements performed on S-II. Moreover, results of S-I are contradicting these observations. Here, matrix crack could only be detected in conjunction with particular excitation motion of [12 mm 5 Hz].

Regarding debonding, similar results were obtained. Here, damage was also detected only at specific excitation modes. In particular, debonding could be detected at excitation amplitudes of 12 mm with all the specimens. Whereas damage detection can be realized successfully if excitations of 3 Hz and 5 Hz are applied in case of S-II, the positive classification of debonding could only be confirmed in connection with 5 Hz excitation frequency in case of S-III. In contrast to this debonding was primarily detected at smaller frequencies of 2 Hz and 3 Hz considering S-I. Best results are obtained in connection with S-II at the particular excitation motion of [15 mm 3 Hz].

Analyzing the results observed on the class of fiber breakage, damage is only sparsely detected among the loading patterns in case of specimens S-I and S-II. Here, fiber breakage is detected exclusively at amplitudes above 12 mm and below 4 Hz. In contrast to this, fiber breakage was frequently detected in case of S-III at excitation amplitudes above 6 mm. Furthermore, using each of the specimens, fiber breakage is detected at [3 Hz 18 mm]. Moreover maximum probability estimation of fiber breakage of 0.95 is achieved at [9 mm 2 Hz] and [12 mm 5 Hz].

According to the experimental results presented in this section, strong dependences of (i) damage detection and (ii) the reliability of the classification result on the excitation motion become evident. Whereas delamination appears to be less sensitive to variable excitations, the classification results of matrix crack, debonding, and fiber breakage strongly vary with the excitation motion. Due to a high degree of variability among specimens and classes, a direct relationship between excitation motion and classification reliability could not be established. Nevertheless, cumulative trends are apparent. Considering the results on matrix crack of the specimens S-I – S-III, improved detectability of damage on increasing frequencies is indicated. Here, damage is detected most frequently in the range of 5 – 6 Hz of



**Table 2.** Probability estimation with respect to excitation motion

excitation frequency. Particularly in case of S-III, this trend appears most pronounced. In case of S-II, improved results are obtained in combination with excitation of [18 mm 6 Hz], whereas regarding S-I matrix crack is only detected at excitation frequency of 5 Hz. Regarding debonding, again a unclear situation appears. Here, detection can be successfully realized at excitation frequencies of 5 Hz with all the specimens. However, debonding is more frequently detected at excitation frequencies of 2 Hz and 3 Hz. Similarly, good reliability of the classification with respect to fiber breakage is primarily achieved at lower frequencies. Considering S-I and S-II, fiber breakage is only detected at excitation frequencies of 2 Hz and 3 Hz in conjunction with large amplitudes. In contrast to this, the classification reliability of fiber breakage appears to be less sensitive to the excitation motion in case of S-III, where best results are also achieved in the range of low excitation frequencies. Similar findings are reported by the results of Gagar,<sup>27</sup> where influences on the activation of AE source-mechanisms are investigated using different aluminum specimens under cyclic loading conditions. Here, large scattering of the AE waveform features under identical test conditions is

observed. Furthermore, these results indicate cumulative trends in AE source activation with respect to loading conditions.

## Discussion

Viewing the results considering the reliability of SHM systems, the question rises, which method can be used to evaluate the reliability of SHM systems. In the past, several ideas have been reported which address different aspects to adopt POD philosophy to SHM applications. For instance, in contrast to conventional NDT the results of SHM systems are statistically not independent due to high acquisition rates.<sup>21</sup> In this context, Schubert Kabban et al. proposed a new methodology to adopt POD procedures to provide compatibility with dependent measurement data, which is obtained from SHM systems.<sup>21</sup> Furthermore, multiple approaches developed to assess the reliability of SHM systems are summarized by Mandache et al.<sup>25</sup> In particular, time-based POD is proposed to address the effect of damage evolution.<sup>25</sup> It is suggested to find a formulation of the POD, which enables stating the probability of

detecting specific defect growth within a given time interval. Multi-dimensional POD is proposed to take the effect of several in-situ effects, i.e. loading conditions, on SHM reliability into account.<sup>25</sup> This includes the computation of POD with respect to each influencing factor to determine the actual reliability of the SHM system in particular situations. However, the approach requires availability of quantitative information on each influencing factor. Furthermore, quantitative knowledge regarding the impact of in-situ effects on the reliability is necessary. In order to minimize the experimental effort required to determine POD, model-assisted approaches can be used.<sup>20</sup> Cobb et al. proposed a model-assisted approach for determining POD of crack detection in aluminum specimens using in-situ ultrasonic inspection technique.<sup>26</sup> Moreover, Eckstein et al. proposed a methodology to quantify SHM performance by using cumulative distribution functions to establish a probabilistic relationship between the detected and real damage size.<sup>47</sup> From this representation, multiple metrics of SHM performance, such as minimum detectable damage size to define a lower bound of POD as accuracy of the inspection method, and probability of false alarm are derived. However, identification of the underlying distribution functions is – particularly in context of in-situ inspection techniques, where a posteriori verification of real damage size is usually not possible – still an open issue.

From the aforementioned approaches to SHM reliability assessment it is noticeable, that the common weak point is characterized by missing detailed knowledge about the impact of different factors on SHM related reliability properties. In this context, especially the experimentally shown results from the previous section states, that the loading (which is unknown in practice) strongly effects the detectability of defects as well as the distinguishability of different damages. However, large scattering of the results prevents the establishment of a direct relationship, which strongly aggravates the online monitoring as well as the verification of healthy states.

## Summary and outlook

Composite materials provide several advantages in many engineering applications. However, the more extensive use is currently restricted because safety and reliability requirements can not be met due to complex damage modes. Therefore, the diagnosis of composite material was chosen as a showcase of SHM due to its practical relevance. Reliability assessment of supervised SHM systems is an open issue which is to be solved before SHM comes into practice.

In this work, a damage classification scheme is used and experimental results were discussed with respect to their reliability. For this purpose, a mechanical test rig is used to subject specimens to various cyclic loading patterns. During loading of the specimens AE measurements are performed. Furthermore, STFT and SVM are employed for extraction of time-frequency domain features from time-series data and classification of the measurement results.

Two different types of experiments were performed to investigate influences on the classification performance. At first, constant excitations were used to assess the reproducibility of the classification results. Here, considerable spreading of the reliability at different points in time is observed despite identical experimental conditions. Partly, this is attributed to the non-deterministic nature of the AE inspection technique, which is only capable to detect damage in-situ. Impact of the excitation motion is indicated, as improved reproducibility is observed in connection with increased load intensity. Significant effects of damage evolution could not be confirmed throughout these experiments.

Hereafter, experiments were performed using variable excitation motions. From the experimental results it becomes evident, that the performance of the classifier strongly depends on the excitation motion. However, a direct relationship could not be established due to large spreading of the classification results among multiple specimens of identical structure, partly leading to contradicting observations. Based on the chosen example related to fault detection and damage discrimination in CFRP material, the large scattering of the classification reliability under identical testing conditions is identified a major challenge in the context of reliability assessment of SHM systems.

## Funding

This research received no specific grant from any funding agency in the public, commercial, or not-for-profit sectors.

## Declaration of conflicting interests

The Authors declare that there is no conflict of interest.

## References

1. Pérez MA, Gil L and Oller S. Impact damage identification in composite laminates using vibration testing. *Composite Structures* 2014; 108(1): 267–276.
2. Agarwal BD, Broutman LJ and Chandrashekhara K. *Analysis and performance of fiber composites*. John Wiley & Sons, 2006.

3. Crivelli D, Guagliano M, Eaton M et al. Localisation and identification of fatigue matrix cracking and delamination in a carbon fibre panel by acoustic emission. *Composites Part B: Engineering* 2015; 74: 1–12.
4. Farrar CR and Worden K. An introduction to structural health monitoring. *Philosophical transactions Series A, Mathematical, physical, and engineering sciences* 2007; 365(1851): 303–315.
5. Gagar D, Martinez M and Foote P. Development of Generic Methodology for Designing a Structural Health Monitoring Installation Based on the Acoustic Emission Technique. *Procedia CIRP* 2014; 22: 103–108.
6. Miller RK and McIntire P. *Nondestructive Testing Handbook: Acoustic emission testing*. American Society for Nondestructive Testing, 1987.
7. Marec A, Thomas JH and El Guerjouma R. Damage characterization of polymer-based composite materials: Multivariable analysis and wavelet transform for clustering acoustic emission data. *Mechanical Systems and Signal Processing* 2008; 22(6): 1441–1464.
8. Crivelli D, Guagliano M and Monici A. Development of an artificial neural network processing technique for the analysis of damage evolution in pultruded composites with acoustic emission. *Composites Part B: Engineering* 2014; 56: 948–959.
9. de Oliveira R and Marques A. Health monitoring of FRP using acoustic emission and artificial neural networks. *Computers & Structures* 2008; 86: 367–373.
10. Hamdi SE, Le Duff A, Simon L et al. Acoustic emission pattern recognition approach based on Hilbert-Huang transform for structural health monitoring in polymer-composite materials. *Applied Acoustics* 2013; 74(5): 746–757.
11. McCrory JP, Al-jumaili SK, Crivelli D et al. Damage classification in carbon fibre composites using acoustic emission: A comparison of three techniques. *Composites Part B* 2015; 68: 424–430.
12. Prosser WH. Waveform analysis of AE in composites. In *Proceedings of the Sixth International Symposium on Acoustic Emission From Composite Materials*. pp. 61–70.
13. Gutkin R, Green CJ, Vangrattanachai S et al. On acoustic emission for failure investigation in CFRP: Pattern recognition and peak frequency analyses. *Mechanical Systems and Signal Processing* 2011; 25(4): 1393–1407.
14. Liu P, Chu J, Liu Y et al. A study on the failure mechanisms of carbon fiber/epoxy composite laminates using acoustic emission. *Materials & Design* 2012; 37: 228–235.
15. Godin N, Hugué S and Gaertner R. Integration of the Kohonen's self-organising map and k-means algorithm for the segmentation of the AE data collected during tensile tests on cross-ply composites. *NDT & E International* 2005; 38(4): 299–309.
16. de Groot PJ, Wijnen PA and Janssen RB. Real-time frequency determination of acoustic emission for different fracture mechanisms in carbon/epoxy composites. *Composites Science and Technology* 1995; 55(4): 405–412.
17. Bussiba A, Kupiec M, Ifergane S et al. Damage evolution and fracture events sequence in various composites by acoustic emission technique. *Composites Science and Technology* 2008; 68(5): 1144–1155.
18. Staszewski W. Intelligent signal processing for damage detection in composite materials. *Composites Science and Technology* 2002; 62(7-8): 941–950.
19. Das S, Srivastava AN and Chattopadhyay A. Classification of damage signatures in composite plates using one-class svms. In *Aerospace Conference, 2007 IEEE*. IEEE, pp. 1–19.
20. Kurz JH, Jüngert A, Dugan S et al. Reliability considerations of NDT by probability of detection (POD) determination using ultrasound phased array. *Engineering Failure Analysis* 2013; 35: 609–617.
21. Schubert Kabban CM, Greenwell BM, DeSimio MP et al. The probability of detection for structural health monitoring systems: Repeated measures data. *Structural Health Monitoring* 2015; 14(3): 252–264.
22. Cai Y, Chow MY, Lu W et al. Evaluation of distribution fault diagnosis algorithms using roc curves. In *Power and Energy Society General Meeting, 2010 IEEE*. IEEE, pp. 1–6.
23. Majnik M and Bosnić Z. ROC analysis of classifiers in machine learning: A survey. *Intelligent Data Analysis* 2013; 17(3): 531–558.
24. Trafalis TB, Adrianto I and Richman MB. Active learning with support vector machines for tornado prediction. In *Computational Science–ICCS 2007*. Springer, 2007. pp. 1130–1137.
25. Mandache C, Genest M, Khan M et al. Considerations on Structural Health Monitoring Reliability. In *International Workshop Smart Materials, Structures & NDT in Aerospace*.
26. Cobb AC, Fisher J and Michaels J. Model-Assisted Probability of Detection for Ultrasonic Structural Health Monitoring. In *4th European-American Workshop on Reliability of NDE*.
27. Gagar D, Foote P and Irving P. Effects of loading and sample geometry on acoustic emission generation during fatigue crack growth: Implications for structural health monitoring. *International Journal of Fatigue* 2015; 81: 117–127.
28. Scruby CB. An introduction to acoustic emission. *Journal of Physics E: Scientific Instruments* 2000; 20(8): 946–953.
29. Al-Jumaili SK, Holford KM, Eaton MJ et al. Parameter Correction Technique (PCT): a novel method for Acoustic Emission Characterisation in Large-Scale Composites. *Composites Part B: Engineering* 2015; : doi:

- 10.1016/j.compositesb.2015.01.044.
30. Fasana A and Garibaldi L. Measurement of Acoustic Emission Signals: Influence of the Couplant. *Key Engineering Materials* 2007; 347: 375–380.
  31. Theobald P, Zeqiri B and Avison J. Couplants and their influence on AE sensor sensitivity. *Journal of Acoustic Emission* 2008; 26: 91–97.
  32. Bohse J. Acoustic emission characteristics of micro-failure processes in polymer blends and composites. *Composites Science and Technology* 2000; 60(8): 1213–1226.
  33. Suzuki M, Nakanishi H, Iwamoto M et al. Application of static fracture mechanisms to fatigue fracture behavior of class a-smc composite. In *Japan-U. S. Conference on Composite Materials, 4 th, Washington, DC*. pp. 297–306.
  34. Worden K, Farrar CR, Manson G et al. The fundamental axioms of structural health monitoring. In *Proceedings of the Royal Society of London A: Mathematical, Physical and Engineering Sciences*, volume 463. The Royal Society, pp. 1639–1664.
  35. Bahoura M and Ezzaidi H. FPGA Implementation of a Feature Extraction Technique based on Fourier Transform. In *Conference on Microelectronics (ICM)*. 24, IEEE, pp. 1–4.
  36. Mertins A. *Signaltheorie*. Springer-Verlag, 2013.
  37. Burges C. A Tutorial on Support Vector Machines for Pattern Recognition. *Data Mining and Knowledge Discovery* 1998; 2(2): 121–167.
  38. Chaplot S, Patnaik L and Jagannathan N. Classification of magnetic resonance brain images using wavelets as input to support vector machine and neural network. *Biomedical Signal Processing and Control* 2006; 1(1): 86–92.
  39. Tan K, Teoh E, Yu Q et al. A hybrid evolutionary algorithm for attribute selection in data mining. *Expert Systems with Applications* 2009; 36(4): 8616–8630.
  40. Samanta B. Gear fault detection using artificial neural networks and support vector machines with genetic algorithms. *Mechanical Systems and Signal Processing* 2004; 18(3): 625–644.
  41. Yin Z and Hou J. Recent advances on SVM based fault diagnosis and process monitoring in complicated industrial processes. *Neurocomputing* 2015; : 1–8.
  42. Lin CJ, Hsu CW and Chang CC. A practical guide to support vector classification. Technical report, Department of Computer Science, National Taiwan University, 2003.
  43. Pollock A. Probability of Detection for Acoustic Emission. *Journal of Acoustic Emission* 2007; 25: 231–237.
  44. Chang CC and Lin CJ. LIBSVM: A library for support vector machines. *ACM Transactions on Intelligent Systems and Technology* 2011; 2: 27:1–27:27. Software available at <http://www.csie.ntu.edu.tw/~cjlin/libsvm>.
  45. Bak KM, KalaiChelvan K, Vijayaraghavan G et al. Acoustic emission wavelet transform on adhesively bonded single-lap joints of composite laminate during tensile test. *Journal of Reinforced Plastics and Composites* 2012; 32(2): 87–95.
  46. Hamstad MA. A review: Acoustic emission, a tool for composite-materials studies. *Experimental Mechanics* 1986; 26(1): 7–13.
  47. Eckstein B, Fritzen C and Bach M. Considerations on the Reliability of Guided Ultrasonic Wave-Based SHM Systems for CFRP Aerospace Structures . In *6th European Workshop on Structural Health Monitoring*, Dresden, Germany, July 3-6, 2012.